JACS
JOURNAL OF THE AMERICAN CHEMICAL SOCIETY
Article
pubs.acs.org/JACS

How Do Disorder, Reorganization, and Localization Influence the Hole Mobility in Conjugated Copolymers?

Sebastian T. Hoffmann,[†] Frank Jaiser,[‡] Anna Hayer,[§] Heinz Bässler,[†] Thomas Unger,[†,‡] Stavros Athanasopoulos,[†,∥] Dieter Neher,[‡] and Anna Köhler*[,†]

[†]Experimental Physics II and Bayreuth Institute of Macromolecular Research (BIMF), University of Bayreuth, Universitätsstr. 30, 95440 Bayreuth, Germany

[‡]Soft Matter Physics, Institute of Physics and Astronomy, University of Potsdam, Karl-Liebknecht-Str. 24-25, 14476 Potsdam-Golm, Germany

[§]Merck KGaA, Frankfurter Str. 250, 64293 Darmstadt, Germany

[∥]Cavendish Laboratory, JJ Thomson Avenue, Cambridge CB3 0HE, United Kingdom

Supporting Information

ABSTRACT: In order to unravel the intricate interplay between disorder effects, molecular reorganization, and charge carrier localization, a comprehensive study was conducted on hole transport in a series of conjugated alternating phenanthrene indenofluorene copolymers. Each polymer in the series contained one further comonomer comprising monoamines, diamines, or amine-free structures, whose influence on the electronic, optical, and charge transport properties was studied. The series covered a wide range of highest occupied molecular orbital (HOMO) energies as determined by cyclovoltammetry. The mobility, inferred from time-of-flight (ToF) experiments as a function of temperature and electric field, was found to depend exponentially on the HOMO energy. Since possible origins for this effect include energetic disorder, polaronic effects, and wave function localization, the relevant parameters were determined using a range of methods. Disorder and molecular reorganization were established first by an analysis of absorption and emission measurements and second by an analysis of the ToF measurements. In addition, density functional theory calculations were carried out to determine how localized or delocalized holes on a polymer chain are and to compare calculated reorganization energies with those that have been inferred from optical spectra. In summary, we conclude that molecular reorganization has little effect on the hole mobility in this system while both disorder effects and hole localization in systems with low-lying HOMOs are predominant. In particular, as the energetic disorder is comparable for the copolymers, the absolute value of the hole mobility at room temperature is determined by the hole localization associated with the triarylamine moieties.

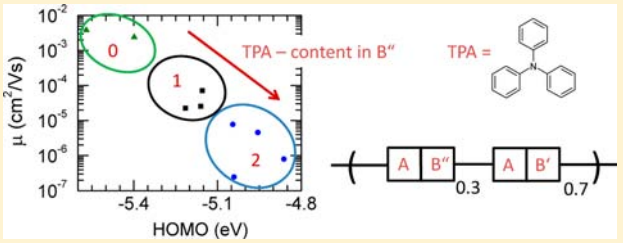

1. INTRODUCTION

The active elements of organic opto-electronic devices such as organic light-emitting diodes (OLEDs), field effect transistors (OFETs), or solar cells are often conjugated polymer films prepared from solution.[1−6] The associated structural randomness inevitably causes some roughening of the energetic landscape in which charge carriers move.[7] As a consequence, their mobility can be some orders of magnitude lower than in crystalline counterpart structures.[8−11] The distinguishing parameter is the degree of built-in energetic disorder. A direct measure of this is the inhomogeneous broadening of the absorption and photoluminescence spectra.[12−14] Build-in disorder controls, for instance, the motion of neutral excited states of singlet[15] or triplet character.[16] In the case of charge transport, one has to rely on indirect methods because in organic solids the oscillator strength of a direct transition from the valence to a conduction state is vanishingly small. An assessment of the roughness of the landscape relevant for charge transport is provided by an analysis of the dependence of charge carrier mobility on temperature and electric field employing theoretical models. Frequently used models are the Gaussian disorder model (GDM)[17] and the correlated disorder model (CDM).[18−20] The GDM rests on the notion that charge carriers hop randomly between sites whose energies form an uncorrelated Gaussian distribution (DOS) while in the CDM concept site correlation is taken care of. A measure of the degree of disorder is the standard deviation σ of the Gaussian DOS. Contributions come from the coupling of a charge carrier residing on a transporting site to induced and, if existing, permanent dipoles in its vicinity. In conjugated polymers, the statistical variation of the conjugation length of the structural units also contributes.[14]

Upon charging a molecule or a subunit of a conjugated polymer, the electron distribution changes. This gives rise to structural reorganization, and as a consequence, the charge

Received: September 10, 2012
Published: January 9, 2013

dx.doi.org/10.1021/ja308820j | J. Am. Chem. Soc. 2013, 135, 1772−1782

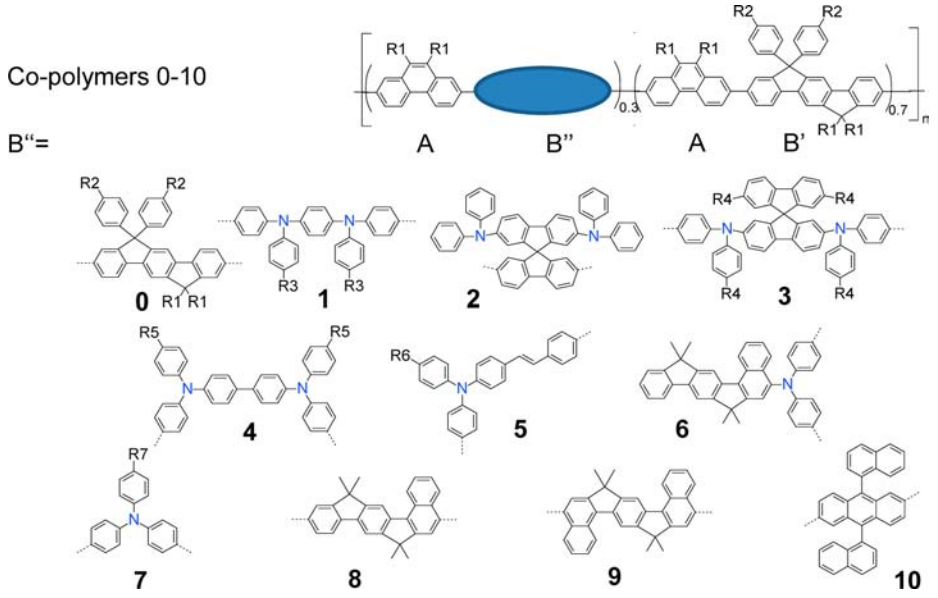

Figure 1. Chemical structures of the copolymers investigated. The copolymers are alternating between A and B, with B being either B′ or B″. The probability of B being B′ is 70% and being B″ is 30%.

transport may become polaronic in nature.[4,21−24] According to Marcus theory, the activation energy E_a for charge transfer between chemically identical molecules can be written as $E_a = (^1/_4)\lambda_{reorg,CT}$ with $\lambda_{reorg,CT}$ describing the energy of the geometric reorganization of the entire system upon charge transfer. Note that the *reorganization* energy for transferring a charge from one site to the next is twice the geometric *relaxation* energy upon ionization of one molecule, $\lambda_{rel,ion}$, since first the donor molecule changes from charged into a neutral state and then the acceptor molecule changes from a neutral to a charged state. This leads to[1,25]

$$E_a = \frac{1}{4}\lambda_{reorg,CT} \cong \frac{1}{2}\lambda_{rel,ion} \quad (1)$$

The interplay between disorder and reorganization effects regarding charge transport has been treated theoretically, but in practice, both contributions are difficult to disentangle.[26,27] In principle, disorder and polaronic effects carry different temperature dependencies—the former yielding a ln μ versus $(1/T)^2$ dependence while the latter follows an Arrhenius law—but owing to the usually limited temperature regime, it is often difficult to split the experimentally measured activation energy into these two contributions unless independent information is available. In the current work, we combine charge transport studies with optical spectroscopy and calculations based on density functional theory (DFT) to unravel the interplay between disorder, polaronic, and localization effects in a series of conjugated copolymers.

The compounds studied here (Figure 1) are conjugated alternating A−B type copolymers suitable as model compounds for the study of charge carrier mobility. Generally, copolymers have become popular for applications in organic solar cells, light-emitting diodes, and transistors due to the ease by which their electronic properties can be modified.[28−31] The materials studied here are eventually intended as blue emissive components in printed OLED displays. The comonomer unit A is always the phenanthrene derivative shown in Figure 1. The comonomer unit B statistically comprises either the substituted indenofluorene labeled B′ or a unit labeled B″. The resulting copolymer has a structure such as ...−A−B′−A−B′−A−B′−A−B″−A−B′−A−B″−A−B″−A−B′−... or similar. The overall composition of the copolymer is 50% of unit A, 35% of unit B′, and 15% of unit B″, with the percentage referring to molar fractions. While A and B′ are the same for all copolymers, B″ differs as shown in the bottom part of the figure, thus leading to copolymers **1**−**10**. In copolymer **0**, B′ = B″; that is, it comprises only the phenanthrene and the indenofluorene units and serves as a reference compound.

While A and B′ mainly dominate the lowest unoccupied molecular orbital (LUMO) and electron mobility of the copolymers studied here, B″ modifies the energy of the copolymer's highest occupied molecular orbital (HOMO), thus tuning the hole transport properties as well as emission color. To obtain different HOMO energies, we employed chromophores for B″ that comprise diamine groups (copolymers **1**−**4**), a monoamine group (copolymers **5**−**7**), or no triarylamine group (copolymers **8**−**10** and copolymer **0**). This systematic variation allows us to investigate the effect of the widely used triarylamines on the hole transporting properties of a polymer.[32,33] Even though copolymers **0**−**10** are structurally related, they differ in the degree to which they allow for geometric relaxation upon transfer of a charge and in the energetic disorder present in the copolymer films. With these properties, the compounds in Figure 1 form a series well-suited to a careful study on the effects of disorder and reorganization on hole transport.

2. METHODS

2.1. Experimental Section. All copolymers were synthesized using a Suzuki-coupling method as described in ref 34. Structures were confirmed by ^{1}H NMR. Purity was confirmed by trace analysis via inductively coupled plasma mass spectrometry (ICP-MS) checking for traces of monomers (Br, B) and catalyst (Pd, P). The following trace contents were found: Br ≤ 50 ppm, B ≤ 20 ppm, P ≤ 200 ppm, and Pd ≤ 15 ppm. Molecular weights and polydispersities were determined by gel-permeation chromatography calibrated against polystyrene standards. The molecular weights were in the range 200 000−600 000 g/mol, with most polymers between 400 000 and 500 000 g/mol. The polydispersities were in the range 2.8−4.0.

dx.doi.org/10.1021/ja308820j | J. Am. Chem. Soc. 2013, 135, 1772−1782

Table 1. HOMO Energies of Copolymers 0−10, Mean HOMO Energies of Copolymers 1−4, 5−7, 8−10 and the Number of Nitrogen Atoms Contained in a Repeat Unit

copolymer	0	1	2	3	4	5	6	7	8	9	10
HOMO (eV)	−5.58	−4.86	−5.04	−4.96	−5.05	−5.21	−5.16	−5.15	−5.54	−5.40	−5.56
mean HOMO (eV)			−5.0 ± 0.1				−5.2 ± 0.05			−5.5 ± 0.1	
nitrogen atoms	0	2	2	2	2	1	1	1	0	0	0

The HOMO levels of the copolymers were determined by cyclovoltammetry measurements in dichloromethane solution using a ECO μAUTOLAB type III potentiostat and a three electrode setup with a rotating gold electrode as the working electrode, a platinum counter electrode, and a reference electrode of Ag/AgCl (3 M KCl). Tetrabutylammoniumhexafluorophosphate at 0.11 M in dichloromethane served as the conducting salt, and tetramethylammonium chloride at 0.4 M in ethylene glycol served as the electrolyte. The redox pair ferrocene/ferrocenium was used as the internal standard.

For hole transport measurements with time-of-flight (ToF), thick polymer films (thicknesses ranging from 2 to 3 μm) were prepared by spin coating from toluene solutions at concentrations between 25 and 50 g/L, depending on the polymer, at a speed of 1000 rpm for 60 s onto glass substrates with prepatterned indium−tin oxide electrodes. A 100 nm thick aluminum electrode was thermally evaporated onto the polymer. The active pixel area was about 2 mm^2. The transport of holes was characterized by the ToF technique as a function of applied electric field and temperature. Charges were generated by approximately 10 ns long pulses of a frequency-tripled Nd/YAG laser (355 nm) at a repetition rate of 10 Hz. Charge carriers were generated by excitation at the high-energy edge of the main absorption band of the polymers. Care was taken that photogeneration occurred only in the first 10% of the film layer by ensuring that the extinction of all polymers at 355 nm was larger than 3 μm^{-1}.Electric fields were applied by a Keithley 237 source measure unit. The transient current signal was amplified using a Femto DHPCA-100 variable range amplifier and recorded with a Yokogawa DL-9040 oscilloscope. The hole mobility was investigated at electric fields between 60 and 450 kV/cm. The range used was limited by signal strength at low fields and leakage currents at high fields. The temperature range was limited from room temperature (approximately 25 °C) to 100 °C. The excitation light was adjusted to low intensities to avoid disturbances due to space charge or other saturation effects during measurements.

Complementary to the ToF experiments, we also measured the mobilities in OFET structures. However, since the data were consistent with the ToF data, they shall not be considered further.

For measurements of absorption and photoluminescence, thin films of about 100 nm thickness were prepared by spin coating from toluene solutions of 15 mg/mL onto Spectrosil B substrates. A Cary5000 ultraviolet visible spectrometer was used to take the absorption spectra. Luminescence spectra at 10 K and at 290 K were taken with the sample placed in a continuous flow helium cryostat. The temperature was controlled using an ITC502 Oxford Intelligent temperature controller. A diode laser at 405 nm (3.06 eV) was used to excite the sample. The emission was recorded with an optical fiber connected to a spectrograph with a CCD camera attached (Oriel MS125 attached to Oriel InstaSpec IV).

The emission spectra were fitted to a Franck−Condon progression in order to derive the disorder parameter σ and the relaxation energy $\lambda_{\mathrm{rel,opt}}$ associated with an emission process. For this, the expression $P(\hbar\omega) = n^3(\hbar\omega)^3\sum_{n_i}((\mathrm{e}^{-S}S_i^{n_i})/(n_i!))\Gamma\delta[\hbar\omega - (\hbar\omega_0 - n_i\hbar\omega_i)]$[35,36] was used, where $P(\hbar\omega)$ is the photoluminescence spectrum in photons/energy interval, $\hbar\omega_0$ is the energy of the 0−0 peak, and $\hbar\omega_i$ are the energies of the vibrational modes i. To obtain the vibrational energies, Raman spectra were taken using a Horiba Labram Raman microscope and exciting the samples with a He−Ne laser at 633 nm. The resulting Raman spectra are displayed in the Supporting Information for reference. For the Franck−Condon progression, it was sufficient to consider five vibrational modes with energies $\hbar\omega_i$ being 1604, 1347, 1202 (or 1255 cm^{-1} for compounds **5** and **9**), 820, and 600 cm^{-1}. n_i = 4 vibrational overtones were taken into account. Γ is the Gaussian line shape operator, $\Gamma = \exp(-(\hbar\omega)^2/2\sigma^2)$, and S_i is the Huang−Rhys parameter for the mode i. The refractive index n was approximated as being constant. Fitting the photoluminescence spectrum yields σ as the standard deviation of the Gaussian line shape and S_i as the Huang−Rhys parameter; the relaxation energy is then obtained as $\lambda_{\mathrm{rel,opt}} = \sum_i S_i\hbar\omega_i$.

2.2. Modeling. To complement the experimental results, we have also performed electronic structure calculations to estimate the reorganization energy for hole transfer for the copolymers of interest and the spatial extent of the polaron state. Internal (inner sphere) reorganization energies were calculated from the adiabatic potential energy surfaces of the neutral and cation states using DFT with the B3LYP hybrid exchange and correlation functional and a split valence 6-31G basis set. B3LYP provides reorganization energies in molecular crystals and single molecules in excellent agreement with the experiment and also rather good values for singlet and triplet excited states in fluorine-based polymers. The inner sphere reorganization energy can be estimated as the energy difference between the vertical ionization potential of the neutral state and the electron affinity of the cation state.[1,23,37] All calculations were performed using the Gaussian 09W program.[38] It should be noted that the computed reorganization energies of the model oligomers in the gas phase provide an upper limit for the internal reorganization energy in the film, since molecular packing and intermolecular interactions impose restrictions, for example, on the torsional relaxation of the polymer when charged. The external (outer sphere) contribution to the reorganization energy, influenced by the local molecular packing, polarization, and electrostatic interactions, has not been considered. Excited-state reorganization energies have been estimated at the time-dependent DFT (TD-DFT) level as $\lambda_{\mathrm{reorg,opt}} = E(S_0 \rightarrow S_1) - E(S_1 \rightarrow S_0)$, where $E(S_0 \rightarrow S_1)$ is the absorption energy for the vertical transition from the ground state S_0 to the first excited state S_1 and $E(S_1 \rightarrow S_0)$ is the emission energy from S_1 to S_0 at the excited-state optimized geometry.

To quantify the extent of hole delocalization, we have calculated the Kohn−Sham lowest singly unoccupied molecular orbital (LSUMO), the orbital resulting from the splitting of the HOMO upon removal of an electron from the molecule. Since, in the gas phase, the B3LYP exchange and correlation (XC) functional overestimates delocalization,[39−41] we have tested four additional hybrid and long-range XC functionals. That is, besides B3LYP, we considered BHandHLYP, a hybrid functional with 50% exact Hartree−Fock (HF) exchange, HSE1PBE, a hybrid functional with short-range HF exchange and long-range DFT exchange, CAM-B3LYP, a long-range corrected hybrid functional with 19% exchange at short-range and 65% exchange at long-range, and LC-wPBE, a long-range corrected functional with exchange from 0% to100%.

Furthermore, we calculated the inverse participation ratio (IPR) of the positive polaron state. This quantity is a commonly used measure in condensed matter theory to characterize the spatial extent of electronic eigenfunctions in disordered systems and provides information on the probability of the quantum state to reside at a given site.[42] The IPR takes a value of unity if the wave function is localized on a single site and it approaches $1/N$ for an extended state uniformly distributed between N sites. The IPR of the polaron state (LSUMO) with eigenvalue E is defined as $\mathrm{IPR}(E) = \sum_{n=1}^{N} q_n^2(E)$, where q_n is the Mulliken atomic charge for the site n, E is the energy of the state, and $\sum_{n=1}^{N} q_n(E) = 1$. A single orbital description of the polaron state offers a simple picture for the extent of the polaron, but the accommodation of the excess charge $+e$ will carry a response from all occupied molecular levels.[40] We have therefore also calculated an inverse participation ratio from the excess atomic charges Δq,

dx.doi.org/10.1021/ja308820j | J. Am. Chem. Soc. 2013, 135, 1772−1782

IPR(Δq) = $\sum_{n=1}^{N}\Delta q_n^2$, with Δq_n the excess atomic charge for the site n given as the difference between the gross atomic charge of the optimized cation state and the gross atomic charge of the optimized neutral state. Gross atomic charges have been calculated from a Lowdin population analysis.

3. RESULTS AND ANALYSIS

3.1. Dependence of Hole Mobility on Amine-Containing Units. In this study, we aim to understand how and why the chemical structures of copolymers **1**−**10** correlate with their hole mobilities. We have therefore first determined the HOMO energies and the room temperature hole mobilities of the entire set of compounds. The HOMO energies obtained from the cyclovoltammetry are listed in Table 1. They show a clear correlation with the number of nitrogen atoms in B″. For copolymers with a B″ unit containing diamines, monoamines, or no nitrogen atoms, we find a mean HOMO level of −5.0, −5.2, and −5.5 eV, respectively. Hole mobilities measured by ToF were in the range of 10^{-6} cm^2/(V s) to 10^{-2} cm^2/(V s); that is, they cover 4 orders of magnitude. Comparison between μ(295 K) and the HOMO position shows that, with the exception of polymer **2**, the room temperature mobility decreases approximately exponentially with the upward shift of the HOMO (see Figure 2). Given this almost continuous

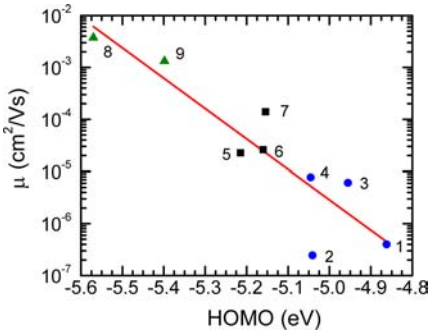

Figure 2. The room-temperature mobility at a field of 3×10^5 V cm^{-1} measured by ToF as a function of the HOMO levels for copolymers **1**−**4** (blue circles), **5**−**7** (black squares), and **8** and **9** (green triangles). The mobility of copolymer **10** exceeded the time resolution of our setup. The red solid line serves to guide the eye.

decrease of the hole mobility with increasing HOMO position, and considering that the introduction of units B″ dissimilar to B′ raise the HOMO energy, one might propose that B″ acts as local hole traps with the trap energy depending on the concrete chemical structure of B″.[43,44] In this case, hole transport would be limited by detrapping of holes from the B″ units back to the phenanthrene−indenofluorene copolymer backbone. We will prove in the following that this scenario is not applicable to the copolymers studied here.

A general expression for the temperature dependence of the mobility μ in the zero field limit in amorphous films is given by[16,25]

$$\mu(T) = \mu_0 \exp\left[-\frac{E_a}{kT} - C\left(\frac{\sigma}{kT}\right)^2\right] \quad (2)$$

where E_a is the activation energy that results from the molecular reorganization energy associated with transferring a charge, $\lambda_{reorg,CT}$, while the parameter σ quantifies the width of the Gaussian distribution of HOMO energies. E_a and σ are thus parameters characterizing polaronic and disorder controlled transport, respectively. The constant C weights the relative contribution of both modes of transport and depends on the ratio σ/E_a. For $E_a \to 0$, C converges to 0.44 ($=(2/3)^2$).[17] For σ = 80 meV and E_a = 75 meV, Parris et al. deduced C = 0.31.[45] Meanwhile, we performed additional Monte Carlo simulations to determine C as a function of σ/E_a that show that, for the experimentally relevant case of $\sigma/E_a \sim 2$, C is close to 0.4.

The decrease in μ(295 K) with increasing HOMO energies may therefore be related either to the prefactor mobility μ_0, that is, the mobility extrapolated to infinite temperature, or to a change in the exponential factor. Distinguishing between both possibilities requires measuring the temperature and field dependence of μ. To this end, we selected four compounds covering a broad range of HOMO levels. The compounds chosen are **1**, **3**, **7**, and **9**. Copolymers **1** and **3** both comprise diamine units but with rather different chemical structure, copolymer **7** has a monoamine hole transport unit, and copolymer **9** is amine-free.

Figure 3a shows a set of ToF signals at room temperature for **1** parametric in the electric field. The photocurrent transients

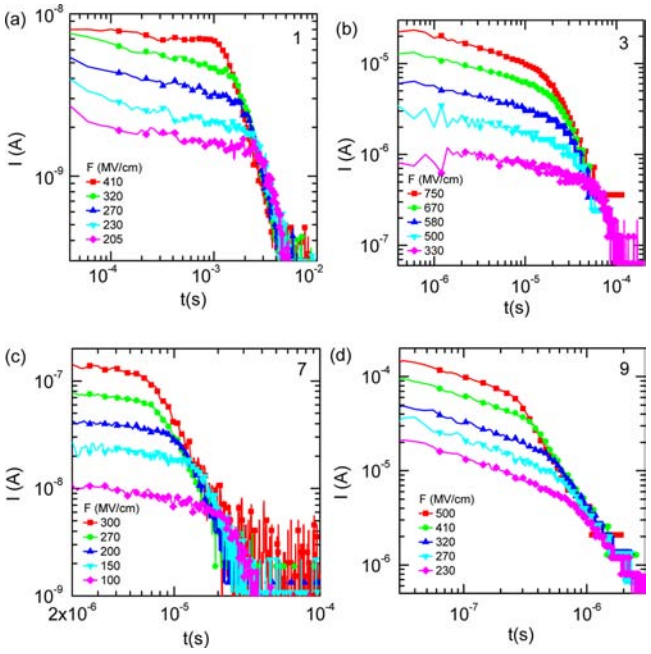

Figure 3. ToF signals at room temperature parametric in electric field for polymers (a) **1**, (b) **3**, (c) **7**, and (d) **9**, plotted on a double-logarithmic scale.

are plotted on a log I versus log t scale. The charge carrier transit times, t_{tr}, are well defined by a sharp kink in the current transients. For $t < t_{tr}$, the current is almost flat, that is, $I(t) \sim t^{-\alpha_1}$ with α_1 = 0.1−0.15, and for $t > t_{tr}$, the current decays as $I(t) \sim t^{-\alpha_2}$ with α_2 = 2.0−2.5. This is characteristic of charge carrier hopping within a Gaussian DOS distribution under moderate energetic disorder, that is, σ/kT < 3.5−4.0.[46,47] The weak decrease of the pretransit current is a signature of the fact that the charge carrier has not yet fully relaxed to quasi-equilibrium. Compounds **3** and **7**, shown in Figure 3b and c, behave similarly. The ToF signals of compound **9** (Figure 3d) are more dispersive. The pretransit current obeys a $I(t) \sim t^{-0.4}$ law while $I(t > t_{tr}) \sim t^{-1.9}$. This is considered as an indication that some charge carriers are lost by weak trapping while their majority reaches the counterelectrode without suffering trapping. Note

dx.doi.org/10.1021/ja308820j | J. Am. Chem. Soc. 2013, 135, 1772−1782

that **9** is the material with the deepest-lying HOMO and is therefore most vulnerable to trapping. The field-dependent mobility can be derived from the charge carrier transit times t_{tr} by $t_{tr} = d/\mu F$, where d is the sample thickness and F is the electric field. Similar ToF signals were obtained at 320, 340, and 350 K. The resulting mobilities are shown in Figure 4 as a

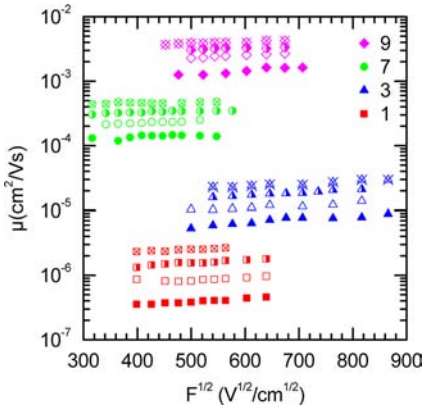

Figure 4. Field dependence of the ToF mobility for compounds **1** (red squares), **3** (blue triangles), **7** (green circles), and **9** (magenta diamonds) at room temperature (filled), 320 K (open), 340 K (half filled), and 350 K (crossed symbols).

function of the square root of the field. The mobility $\mu(F)$ shows a Poole–Frenkel-like field dependence; that is, $\mu(F) \propto \exp(\gamma\sqrt{F})$. Extrapolating the field-dependence of μ to $F = 0$ yields the zero-field ToF mobilities shown in Figure 5 as a function of temperature.

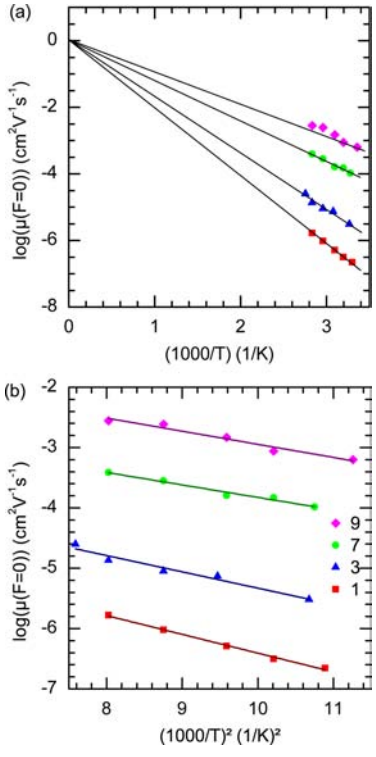

Figure 5. Temperature dependence of the zero-field ToF mobility for compounds **1** (red squares), **3** (blue triangles), **7** (green circles), and **9** (magenta diamonds) plotted (a) as log μ versus $1/T$ and (b) log μ versus $1/T^2$. The black lines represent corresponding fits.

To examine whether the change in mobilities with HOMO energies results from a variation in the prefactor mobility μ_0, from a change in E_a, or from a change in σ, we plot the mobility semilogarithmically against $1/T$ and against $1/T^2$ and fit them to eq 2 for the two limiting cases of presuming entirely polaronic transport ($\sigma = 0$) and entirely disorder controlled transport ($E_a = 0$). As evident in Figure 5, both procedures yield fits of equal quality, since the temperature range of the ToF experiments is only 60–70 K. In the polaronic case ($\sigma = 0$) (Figure 5a), fitting the mobilities to $\mu = \mu_0 \exp(-E_a/kT)$ gives $\mu_0 \cong 1$ V cm^{-1} s^{-1} for all compounds and E_a values ranging from about 180 to 400 meV as detailed in Table 2. Thus, an interpretation of the mobilities in terms of polaronic transport would imply that the electronic coupling between adjacent hopping sites, manifested in μ_0, is the same for all polymers and comparable to those of molecular crystals.[48] Moreover, it would imply that the different room-temperature values of μ result from different reorganization energies. We next consider the fit for the entirely disorder controlled transport ($E_a = 0$) (Figure 5b). Fits to $\mu = \mu_0 \exp(-0.44(\sigma/kT)^2)$ show that the disorder parameters are centered about a mean value of about 100 meV, with a material dependent variation of only ±10 meV. The major difference in the parameters is the prefactor mobility μ_0. In the series **1**, **3**, **7**, and **9**, it increases by a factor of 200, that is, from 0.5×10^{-3} to 91×10^{-3} V cm^{-1} s^{-1} (see Table 2). In the disorder picture, the dependence of the hole mobility on the HOMO position, documented by Figure 2, is due to μ_0 rather than to σ. Consequently, it has to be accounted for by variations in the electronic coupling between the transporting elements of the polymer chain rather than by thermally assisted detrapping from the amine-containing moieties to the phenanthrene–indenofluorene moieties. This analysis shows that an interpretation of the ToF data in a polaronic or a disorder-dominated picture leads to mutually exclusive conclusions, and one cannot decide upon the mode of transport by considering only the quality of fit to the temperature dependence of the hole mobility. Further evidence is required to determine what controls the charge transport.

3.2. Polaron or Disorder Transport. One piece of information useful to assess the mode of transport is the value of the reorganization energy associated with transferring a charge from one chromophore to the next, $\lambda_{reorg,CT}$. Following eq 1, this yields the magnitude of the polaronic contribution. Another helpful value is the magnitude of the disorder parameter σ. We shall now argue that we can use the reorganization energy derived from optical spectra, $\lambda_{reorg,opt}$, to obtain an upper value for the polaronic activation energy E_a and that the optical spectra also reveal information on σ . We have calculated the reorganization energies for transferring a hole from one molecule to the next, $\lambda_{reorg,CT}$, from DFT, as well as the reorganization energy associated with singlet exciton transfer, $\lambda_{reorg,opt} = \lambda_{rel,abs} + \lambda_{rel,PL}$, using TD-DFT for model tetramers to copolymers **1**, **3**, **7**, and **9**. The values obtained are listed in Table 3. As expected, the reorganization energies for hole transfer are significantly lower than those for singlet exciton transfer. The reorganization energies show the same trend in both cases.

These calculations are carried out for the gas phase and thus concern only the *internal* part of reorganization energy, that is, the contribution resulting from the geometric distortions of the electron-donating and the electron-accepting chromophore. In the spin-coated amorphous film, two additional effects need to

dx.doi.org/10.1021/ja308820j | J. Am. Chem. Soc. 2013, 135, 1772–1782

Table 2. Fit Parameters Obtained from Analyzing the Temperature-Dependent ToF Mobilities in Figure 5 according to Eq 2 in a Polaron Model (σ = 0) and in a Disorder Model (E_a = 0), along with the HOMO Levels for Ease of Comparison

model			copolymer **1**	copolymer **3**	copolymer **7**	copolymer **9**
		HOMO (eV)	−4.86	−4.96	−5.15	−5.4
polaron	{	E_a (meV)	178	235	329	397
		μ_0 (cm^2/(V s))	1	1	1	1
disorder	{	σ (meV)	109	102	89	91
		μ_0 (10^{-3} cm^2/(V s))	0.51	2.4	17	91

Table 3. Reorganization Energy for Singlet Exciton Transfer, $\lambda_{reorg,opt}$, and the Deduced Polaronic Activation Energy E_a = $\lambda_{reorg,opt}/4$, as well as $\lambda_{reorg,CT}$ and E_a for Charge Transfer, Derived by DFT and TD-DFT Calculations, Respectively, Using B3LYP[a]

model/copolymer			**1**	**3**	**7**	**9**
DFT charge	{	$\lambda_{reorg,CT}$ (meV)	183	152	100	123
		E_a (meV)	46	38	25	31
TD-DFT exciton	{	$\lambda_{reorg,opt}$ (meV)	845	707	394	453
		E_a (meV)	211	177	98	113
fluorescence exciton	{	$\lambda_{reorg,opt}$ (meV)	344	320	244	310
		E_a (meV)	86	80	61	78

[a]The values of $\lambda_{reorg,opt}$ and E_a derived from an analysis of the thin-film fluorescence spectra are also given.

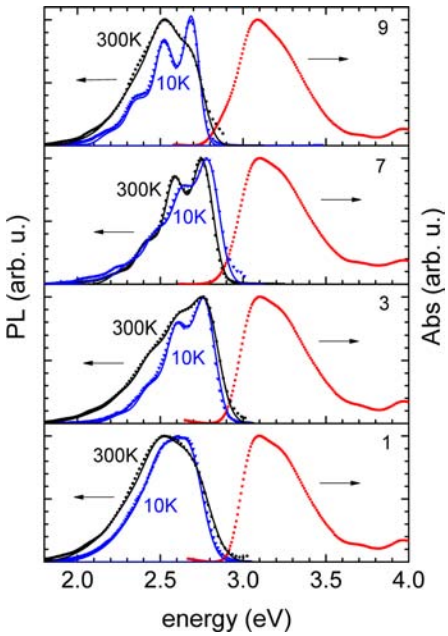

Figure 6. Absorption at 300 K (red squares) and fluorescence at 10 K (blue triangles) and at 300 K (black circles) for compounds **1**, **3**, **7**, and **9**. Franck−Condon fits for the fluorescence spectra at both temperatures are also shown as solid lines.

be considered. First, the polymers are constrained and are less able to distort, thus implying a lower thin-film reorganization energy than calculated for the gas phase. Second, according to Marcus theory, an *external* contribution to the reorganization energy needs to be taken into account.[49] Marcus theory was originally developed for molecules in solution, where the total reorganization energy for the charge transfer was found to include the geometric relaxation of the donor, that of the acceptor, and the energy required to reorient the solvent molecules surrounding donor and acceptor. In an amorphous film, the donor and acceptor chromophores are "dissolved" in other polymer chains. As in solution, the transfer of a charge is associated with a change in the local polarization of the environment. However, in contrast to solution, this does not lead to a significant change in orientation, distance, or geometry of the adjacent polymer segments because their structure is frozen in below the glass transition temperature. The effect of the external contribution on the reorganization energy in solids should therefore be very small, and this is largely confirmed by calculation performed on molecular crystals[50−52] and on disordered films of Alq_3,[53] though we are aware of one differing report.[54] Contrary to the reorganization energy, the polarization effects can lead to a significant energetic disorder in the amorphous film, in particular for short oligomers.[14,55]

From our basic reasoning in combination with the calculations, we see that we can employ the optical spectra to obtain an upper experimental value for the polaronic activation energy E_a in the amorphous film. To obtain the relaxation energies associated with an optical transition, we consider the fluorescence spectra at 300 and 10 K shown in Figure 6. Upon cooling to 10 K, some spectral narrowing occurs that is helpful when subjecting the spectra to a Franck−Condon analysis. Such an analysis reflects the displacement of the oscillator when going from the ground state to the excited state and quantifies it in terms of the Huang−Rhys factor. Taking vibrational modes $\hbar\omega_i$ from the Raman spectra, the fluorescence spectra can be fitted to give the Huang−Rhys factor S_i for each mode. The geometric relaxation energy associated with the fluorescence is then given by $\lambda_{rel,PL} = \sum_i S_i\hbar\omega_i$. As the room-temperature spectra are rather broad, we had fitted the well-resolved 10 K spectra, where the analysis is straightforward, and then modeled the 295 K spectra by employing roughly the same Huang−Rhys factors as at 10 K, yet using a larger inhomogeneous broadening. The reorganization energy derived in this way for singlet exciton transfer $\lambda_{reorg,opt} = \lambda_{rel,abs} + \lambda_{rel,PL} \approx 2\lambda_{rel,PL}$ is listed in Table 3. The values vary between 244 and 344 meV, implying an activation energy for singlet transfer in the range from 61 to 86 meV. A few observations may be noted.

(i) When comparing the values of $\lambda_{reorg,opt}$ (or E_a) derived by theory for the gas phase and by experiment for the film, we see that, for compound **9**, the thin-film value is about 20% lower than the calculated gas-phase value, consistent with a slightly higher degree of rigidity in the solid. This difference becomes larger with increasing content of nitrogen in the structure. We attribute this to the fact that the solid phase constraints the orientation of the phenyl rings and thus limits geometric relaxation of the triarylamine units.

(ii) Comparison of the DFT-based reorganization energies for charges and excitons shows that, for charge transfer, $\lambda_{reorg,CT}$ (and concomitantly E_a) is a factor of 3−4 lower than for exciton transfer. Furthermore, as just discussed,

dx.doi.org/10.1021/ja308820j | J. Am. Chem. Soc. 2013, 135, 1772−1782

the DFT-based energies exceed the experimentally derived ones.

Combining the insight of (i) and (ii), a generously estimated upper limit for the activation energy for polaronic charge transfer is therefore $E_a \leq 40$ meV, that is, about half of the experimental, optically derived activation energy for exciton transfer. One might take the view that it would be better to use a long-range corrected functional that might give larger values, implying a larger polaronic contribution. We have assessed $\lambda_{reorg,opt}$ and $\lambda_{reorg,CT}$ using the long-range corrected functional CAM-B3LYP. The absolute gas-phase values found are indeed larger, yet we still find $\lambda_{reorg,CT} \cong \lambda_{reorg,opt}/3$, so that the general conclusion remains unchanged; that is, $^1/_2$ of the exciton reorganization energy is still a good estimate for the charge reorganization energy. This insight that the optical reorganization energy is correlated to the charge reorganization energy by being very roughly the sum of the hole and electron reorganization energies is not really surprising, given that the optical transition is a simultaneous generation of electrons and holes and consistent with earlier work.[56]

This information can be used to evaluate the appropriateness of a pure polaron model based on experimental data. The activation energies obtained by analyzing the ToF data in a polaron model, shown in Table 2, exceed the values estimated from the optical measurements by a factor of about 5−10. In addition, in a polaron model, the activation energy decreases with nitrogen content in the structure, at variance with the trend found by calculation and fluorescence data. From this quantitative analysis of the reorganization energy, a polaron model does not seem suited to describe the hole transport. A qualitative assessment regarding the importance of the structural relaxation on hole transport is further provided by Figure 7 in which the room temperature hole mobilities are plotted against the experimentally derived reorganization energy $\lambda_{reorg,opt}$.

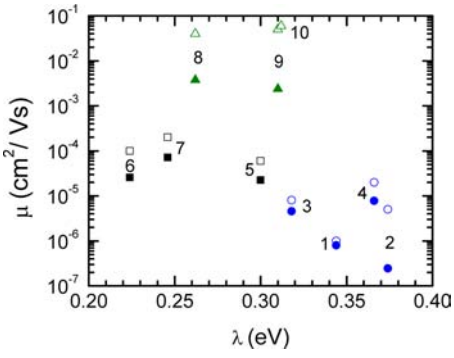

Figure 7. Room-temperature hole mobilities obtained by ToF measurements (solid symbols) and by OFET measurements (open symbols) plotted against the optical reorganization energy $\lambda_{reorg,opt}$.

We next consider what may be learned from the optical spectra regarding the energetic disorder, parametrized through the standard deviation σ of the Gaussian DOS. The room-temperature absorption spectra shown in Figure 6 reveal a low energy tail. Comparing it to a Gaussian line shape indicates a σ of 100−110 meV. This value is remarkably close to the Gaussian width inferred from the analysis of the ToF experiments in the disorder model (Table 2). The fluorescence spectra recorded at 295 K feature a Gaussian high energy tail with a variance of 80−90 meV, indicating that the inhomogeneous broadening in emission at 295 K is about 20% less than in absorption. It turns out that the σ values for absorption are about 10% larger and those for fluorescence are about 10% smaller than the σ values inferred from ToF experiments. By taking the arithmetic mean, optical and electrical values agree. This is a gratifying result because it allows prediction of the width of the hole states from simple spectroscopy. At first glance, such a correspondence is unexpected because those standard deviations are the relative spread of the polarization energies of charge carriers on the one side and of neutral singlet states on the other side. One would surmise that the width of the distribution differs significantly.[17] The reason is likely to be due to the fact that, in the case of conjugated polymers, the dispersion of the energy of both neutral and charged states is mainly caused by the statistical variation of the lengths of the conjugated segments rather than by the spread of the van der Waals energies of either charged or neutral excitations in the surrounding polarizable environment.[14] The latter is the dominant contribution for short oligomers.[14] Thus, considering the results obtained from the absorption and fluorescence spectra, we find values for $E_a \leq 40$ meV and $\sigma \approx 100$ meV that are in agreement with a disorder-based interpretation of the ToF data and that are at variance with a polaron-based analysis.

3.3. What Causes the Variation in Hole Mobilities. It is appropriate to summarize the insight gained so far. We have determined the room-temperature ToF mobilities for a large set of related polymers and found them to depend exponentially on the HOMO energies. The mobility may depend on the coupling between chains, expressed through μ_0, on the geometric reorganization associated with the charge transfer, leading to E_a, or on the energetic disorder in the film, parametrized by σ. To assess whether geometric reorganization or energetic disorder have a significant contribution, we have measured the temperature dependence of the ToF mobility and fitted the data presuming exclusively polaronic ($\sigma = 0$) or exclusively disorder-controlled ($E_a = 0$) transport. Although equally satisfactory fits are obtained, we favor the disorder concept for the following reasons: (i) the σ values inferred from ToF experiments and optical spectra are comparable; (ii) the numbers for E_a required in a polaron model exceed the experimentally determined upper limits by a factor of 5−10, and they show an opposite trend with the number of nitrogen atoms; (iii) there is no correlation between the hole mobilities and the measured/calculated reorganization energies (see Figure 7); and (iv) the prefactor mobilities derived from the polaron model are in a similar range than those of molecular crystals and thus exceed the experimental values for disordered organic materials.[47,57]

Having identified the mode of hole transport, we investigate the reason why the hole mobilities differ by more than 2 orders of magnitude although the disorder parameters are similar. As evident from Table 2, a disorder-controlled hole transport implies that that the prime reason is related to the prefactor mobilities μ_0 and thus the strength of the electronic coupling between the transport sites. Key information is provided by the correlation between μ_0 and the HOMO position in the series of compounds **1**, **3**, **7**, and **9**. (Figure 8). Log μ_0 decreases with the upward shift of the HOMO. This shift correlates with absence or presence of an amine moiety incorporated in the chain. Compound **9** is free of amine, **7** carries a monoamine group, while **3** and **1** contain diamines.

dx.doi.org/10.1021/ja308820j | J. Am. Chem. Soc. 2013, 135, 1772−1782

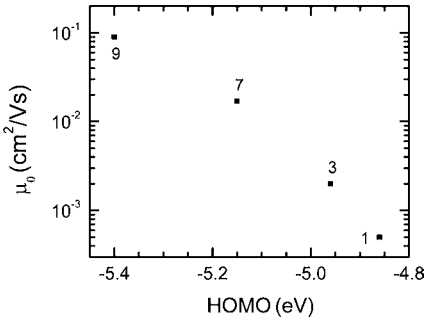

Figure 8. Prefactor ToF mobility μ_0 plotted against the HOMO values for compounds **9**, **7**, **3**, and **1**.

The way by which the amine groups can affect the electronic coupling may be related to the localization of the hole wave function. Since the amine group is electropositive, resulting in a high lying HOMO, it is likely that the positive excess charge will be progressively localized at the amine group. If the wave function of the charged polymer chain becomes more localized, the distance between the transport sites increases. Localization thus implies weaker electronic coupling between the charge carrying moieties, that is, a lower prefactor mobility. This argument obtains further support by the exceptionally low mobility of copolymer **2** (Figure 2). In polymer **2**, the amine moieties do not form part of the conjugated backbone as is the case for the other copolymers. Rather, the amines are located on what amounts to a side chain orthogonal to the polymer backbone; conjugation goes through one side of the spiro group while the amine is in the orthogonal branch. As a result, the hole is fully localized on the side chain. The mobility of this polymer with a fully localized hole is significantly lower than what our trend would predict for the HOMO if the amines were still part of the conjugated backbone. At this stage, it is appropriate to comment on the role morphology plays regarding charge transport. The mobility of charges is known to depend strongly on the degree of crystallinity present in a polymer chain, as is evidenced through many studies of P3HT. The polymers used here are statistical copolymers. Due to their random order and bulky side chains and their deposition by spin coating, it is reasonable to assume an amorphous structure of the thin film. We consider that all copolymers are similarly amorphous. This is confirmed by the fact that the disorder parameter σ, found from the optical absorption data, varies by only about 10% between the different copolymers. If we now find that all copolymers are similarly amorphous, and that the mobility prefactor varies by almost 3 orders of magnitude between them, we can conclude that the average electronic coupling varies. In this work, on the basis of macroscopic experimental data, we conclude on the average degree of localization, the average electronic coupling, and the macroscopic average mobility.

DFT calculations can give some guidance to the degree of hole localization for the gas-phase charged state geometry.

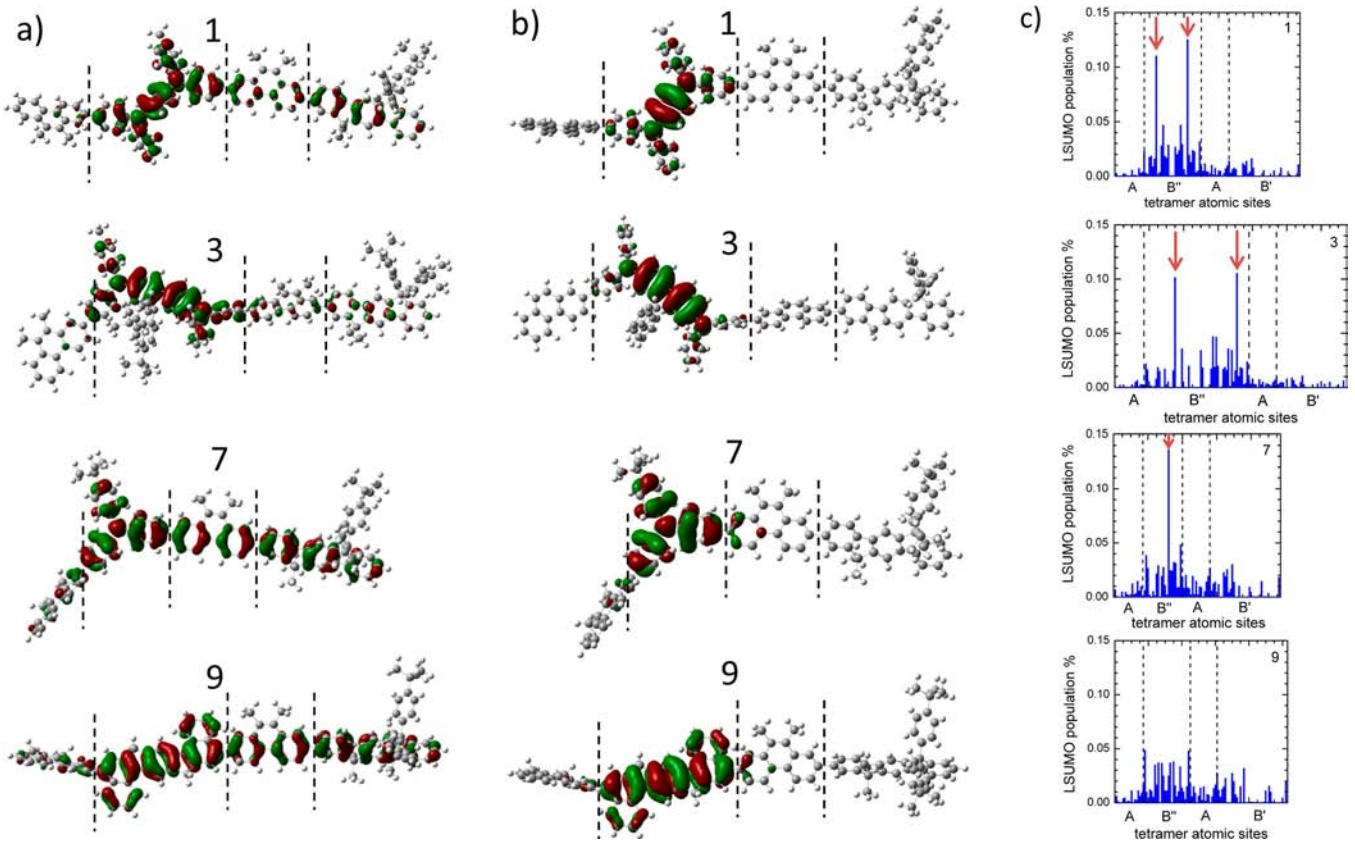

Figure 9. Kohn–Sham LSUMOs of the cation state of a model tetramer A–B″–A–B′ for materials **1**, **3**, **7**, and **9** obtained (a) with B3LYP and (b) with LC-wPBE. (For **3** with LC-wPBE, the methyl groups have been replaced by H as the calculations otherwise never converged). (c) Probability distribution of the LSUMO from atomic populations of the carbon and nitrogen atoms, calculated with B3LYP, for **1**, **3**, **7**, and **9**. Except for the hydrogens, the molecular atoms are labeled consecutively from left to right and listed on the abscissae. For clarity, the tetramer sections A, B″, A, and B′ are indicated and separated by a vertical dashed line. The position of the nitrogens is indicated by an arrow.

dx.doi.org/10.1021/ja308820j | *J. Am. Chem. Soc.* 2013, 135, 1772–1782

Figure 9 depicts a visualization of the calculated Kohn−Sham LSUMOs of positively charged model tetramers for the copolymers **1**, **3**, **7**, and **9**. The LSUMO might be thought as equivalent to the HOMO in a neutral molecule, yet with one charge removed. The tetramers are built in the order A−B″−A−B′ (from left to right), with A being phenanthrene, B″ as indicated in Figure 1, and B′ being indenofluorene. As the degree of delocalization predicted by electronic structure calculations depends strongly on the method used (semi-empirical or DFT) and in the latter case also on the choice of functional, we employed five different functionals. The results obtained for B3LYP and HSE1PBE were very similar and overall of a more delocalized character, while the results for LC-wPBE, CAM-B3LYP, and BHandHLYP formed a second group with a more localized character. Figure 9 shows one set for each group, represented by B3LYP and by LC-wPBE. The strong localization of the orbitals on the two compounds containing diamine units, **1** and **3**, is evident for any choice of functional. However, the orbital on the model tetramer for compound **7** containing one amine visually appears similarly delocalized to **9** when B3LYP is used (Figure 9a), while they seem similarly localized for LC-wPBE (Figure 9b). The same qualitative results were obtained when considering the HOMOs of the neutral oligomers or when calculating the spin density. The surfaces depicted in Figure 9 indicate a three-dimensional profile at which the molecular orbital wave function exceeds an arbitrary, positive or negative fixed value, yet they do not readily indicate by how much the fixed threshold value is surpassed at different positions along the molecule.

To get insight into the visually equal delocalization of the LSUMO for molecules **7** and **9**, we considered the values of the atomic contributions to the LSUMO. In Figure 9c, the abscissa indicates, consecutively from left to right, the carbon and nitrogen atoms of the model tetramers. The four different units of the tetramers, A, B″, A, and B′, are indicated and visually separated by a dashed line. The ordinate denotes the contribution of each atomic site to the discrete probability distribution in the LSUMO for the B3LYP functional. Figure 9c logically supplements Figure 9a. For molecules **1** and **3**, comprising two diphenylamine units, one observes not only that the main contributions to the LSUMO arise mainly from the B″ unit, as already evident in Figure 9a, but also that particularly high contributions are associated with the two nitrogen sites. As expected intuitively, the hole resides most likely on the two nitrogen sites and between them, corresponding to a significant degree of localization. In the case of amine-free molecule **9**, the contributions of different atoms are fairly evenly distributed, implying a more delocalized hole wave function. A widespread of atomic contributions is also observed for the monoamine-containing molecule **7**, yet a significant fraction (14%) of the probability density for the hole is localized on the nitrogen atom, suggesting a quantitatively higher charge localization for **7** compared to **9**. The same trends are found when analyzing the LSUMO atomic contributions for any of the other functionals employed in this study. The degree of delocalization may also be derived from an inverse participation ratio (IPR) analysis, calculated from either the LSUMO atomic charges or from the total excess charge Δq as detailed above in the Methods section. For all functionals employed, we obtain similar trends for both the IPR(LSUMO) and the IPR(Δq) values, with a higher degree of localization for the amine-containing molecules.

Overall, the DFT calculations confirm our reasoning that the electropositive amine group induces a progressive localization of the hole wave function, thus increasing the distance between hopping sites and in this way reducing the electronic coupling.[58] This electronic effect is likely to be enhanced by the large steric demand of the angular and tilted triarylamine group that implies a larger mean distance to adjacent chains than the planar and rigid amine-free units. This localization effect is another manifestation of the profound effect that electronic coupling between charge transporting moieties has.[21,23,59]

DISCUSSION AND CONCLUSIONS

The central question we address is how and why the hole mobility depends on the chemical structure. This requires first identification of the charge transport mechanism. The distinction between various models for charge transport in conjugated polymers and disordered organic semiconductors in general is often made by measuring charge carrier mobility as a function of electric field and temperature. Since the useful temperature range is limited by the glass transition temperature at the high-temperature side and the temperature at which transport becomes dispersive, the experimentally available temperature window can be quite small. For this reason, fitting the $\mu(T)$ dependence based upon various models can become ambiguous. In order to overcome this ambiguity, we investigated the series of conjugated polymers by combining the ToF technique to measure the mobility as a function of temperature and electric field with cyclic voltammetry, optical spectroscopy, and DFT calculations. From the experiments, we determine both the electrically and optically probed density of states distributions. A noteworthy result is that the width of the inhomogeneous broadening of the DOS for neutral excitons and for charges is very similar. This appears to be a characteristic feature of conjugated polymers in which disorder results predominantly from the variation of the conjugation lengths rather than from van der Waals coupling among the chains. This recognition provides an important clue for materials design. The DFT calculations for the reorganization energy provides an upper limit for the hole transfer reorganization energy. In fact, the DFT calculations yield reorganization energies for hole transfer that are by a factor of about 2.5 lower than optically determined values for exciton transfer, absolute values ranging from 25 to 45 meV only. On the basis of the theory of charge transport in a polaronic system in the presence of disorder, we are able to firmly establish that, in our system, hole transport is disorder-controlled. It is obvious that this conclusion cannot be generalized to any excitation on any organic semiconductor because the relative contribution of disorder and polaron effects is dictated by the σ^2/E_a ratio in eq 2, with the disorder parameter entering quadratically. Typical values for the disorder parameter for hole transport in disordered organic semiconductors are on the order of 100 meV, consistent with the value found here. The situation is different for the transport of neutral triplet excitations where σ is typically 30 meV while the E_a values are typically equal or larger for triplets than for charges.[16]

In the manuscript, we show that, even though the mechanism of transport is controlled by energetic disorder, this is not sufficient to account for the variation of room temperature mobility over five decades in a range of chemically related copolymers. Rather, the variation over five decades in the absolute value of the mobility is controlled by the degree of

charge localization associated with the incorporation of triphenylamine units in the chemical structure.[60−64] This is an entirely novel aspect that has not been addressed so far and that relates in particular to copolymers that have become increasingly popular for their use in OLED and solar cell structures. Usually, the discussion is led in terms of polaronic or disorder contributions yet not by contemplating the impact of excited-state delocalization. The paradox insight that triphenylamine moieties, usually incorporated to enable hole injection by their high HOMO level, may actually serve to reduce charge mobility has important bearing on the synthetic design of novel copolymers.

This novel conceptual insight is obtained by the comprehensive approach of taking together measurements of charge transport AND optical spectroscopy and to support the conclusions obtained further by DFT calculations. Such a comprehensive approach has never been attempted so far, to the best of our knowledge. It has also not been possible so far, since the connection between optical spectroscopy and transport properties has only emerged recently (see ref 25) and because such studies require an extensive set of chemically related copolymers that are usually not readily available. The fact that we can use simple absorption measurements to obtain information on transport properties is by the way very valuable for material screening, for example, in an industrial context.

One strategy toward an improvement of the hole mobility would then be to employ homopolymers with amine functionalities or related hole-transporting moieties. If copolymers are desired, the strategy would be to increase the concentration of the amine functionalities.[65] This would enhance electronic coupling and smoothen the intrachain energy landscape. Analogous considerations should apply to films made from blends of low molecular materials, as is demonstrated by the work on molecularly doped polymers.

■ ASSOCIATED CONTENT

Supporting Information

Raman spectra for compounds **1**−**10**. This material is available free of charge via the Internet at http://pubs.acs.org.

■ AUTHOR INFORMATION

Corresponding Author

Anna.koehler@uni-bayreuth.de

Notes

The authors declare no competing financial interest.

■ ACKNOWLEDGMENTS

We thank Dr. Niels Schulte of Merck KGaA for providing the polymers studied in this paper as well as Dr. David Sparrowe of Merck Chemicals Ltd. for the measurement of OFET mobilities. We further acknowledge Christoph Hanske for assistance with the Raman measurements. D.N. acknowledges funding by the Bundesministerium für Bildung und Forschung (BMBF project "NEMO", FKZ 13N10622. A.H. acknowledges funding by the Bundesministerium für Bildung und Forschung (BMBF project "NEMO", FKZ 13N10614). A.K. and T.U. acknowledge funding by the GRK 1640 *Photophysics of Synthetic and Biological Multichromophoric Systems* of the German science foundation (DFG)

■ REFERENCES

(1) Bredas, J. L.; Beljonne, D.; Coropceanu, V.; Cornil, J. *Chem. Rev.* **2004**, *104*, 4971.
(2) Forrest, S. R. *Nature* **2004**, *428*, 911.
(3) Wu, F. I.; Yang, X. H.; Neher, D.; Dodda, R.; Tseng, Y. H.; Shu, C. F. *Adv. Funct. Mater.* **2007**, *17*, 1085.
(4) Gilot, J.; Wienk, M. M.; Janssen, R. A. J. *Nat. Mater.* **2007**, *6*, 704.
(5) Peet, J.; Kim, J. Y.; Coates, N. E.; Ma, W. L.; Moses, D.; Heeger, A. J.; Bazan, G. C. *Nat. Mater.* **2007**, *6*, 497.
(6) Sirringhaus, H.; Tessler, N.; Friend, R. H. *Science* **1998**, *280*, 1741.
(7) Movaghar, B.; Grünewald, M.; Ries, B.; Bässler, H. *Phys. Rev. B* **1986**, *33*, 5545.
(8) Hertel, D.; Bässler, H. *ChemPhysChem* **2008**, *9*, 666.
(9) Bässler, H.; Köhler, A. *Top. Curr. Chem.* **2012**, *312*, 1.
(10) Coehoorn, R. *Phys. Rev. B* **2007**, *75*, 155203.
(11) Grozema, F. C.; Siebbeles, L. D. A. *Int. Rev. Phys. Chem.* **2008**, *27*, 87.
(12) Hoffmann, S. T.; Koenen, J.-M.; Forster, M.; Scherf, U.; Scheler, E.; Strohriegl, P.; Bässler, H.; Köhler, A. *Phys. Rev. B* **2010**, *81*, 115103.
(13) Kador, L. *J. Chem. Phys.* **1991**, *95*, 5574.
(14) Hoffmann, S. T.; Bässler, H.; Köhler, A. *J. Phys. Chem. B* **2010**, *114*, 17037.
(15) Athanasopoulos, S.; Emelianova, E. V.; Walker, A. B.; Beljonne, D. *Phys. Rev. B* **2009**, *80*, 195209.
(16) Hoffmann, S. T.; Athanasopoulos, S.; Beljonne, D.; Bässler, H.; Köhler, A. *J. Phys. Chem. C* **2012**, *116*, 16371.
(17) Bässler, H. *Phys. Status Solidi B* **1993**, *175*, 15.
(18) Gartstein, Y. N.; Conwell, E. M. *Chem. Phys. Lett.* **1994**, *217*, 41.
(19) Dunlap, D. H.; Parris, P. E.; Kenkre, V. M. *Phys. Rev. Lett.* **1996**, *77*, 542.
(20) Tanase, C.; Meijer, E. J.; Blom, P. W. M.; de Leeuw, D. M. *Phys. Rev. Lett.* **2003**, *91*, 216601.
(21) Hutchison, G. R.; Ratner, M. A.; Marks, T. J. *J. Am. Chem. Soc.* **2005**, *127*, 16866.
(22) Vehoff, T.; Chung, Y. S.; Johnston, K.; Troisi, A.; Yoon, D. Y.; Andrienko, D. *J. Phys. Chem. C* **2010**, *114*, 10592.
(23) Coropceanu, V.; Cornil, J.; da Silva, D. A.; Olivier, Y.; Silbey, R.; Bredas, J. L. *Chem. Rev.* **2007**, *107*, 926.
(24) Schein, L. B.; Glatz, D.; Scott, J. C. *Phys. Rev. Lett.* **1990**, *65*, 472.
(25) Köhler, A.; Bässler, H. *J. Mater. Chem.* **2011**, *21*, 4003.
(26) Kreouzis, T.; Poplavskyy, D.; Tuladhar, S. M.; Campoy-Quiles, M.; Nelson, J.; Campbell, A. J.; Bradley, D. D. C. *Phys. Rev. B* **2006**, *73*, 235201.
(27) Khan, R. U. A.; Poplavskyy, D.; Kreouzis, T.; Bradley, D. D. C. *Phys. Rev. B* **2007**, *75*, 035215.
(28) Nielsen, C. B.; Ashraf, R. S.; Schroeder, B. C.; D'Angelo, P.; Watkins, S. E.; Song, K.; Anthopoulos, T. D.; McCulloch, I. *Chem. Commun.* **2012**, *48*, 5832.
(29) Siram, R. B. K.; Smith, J.; Anthopoulos, T. D.; Patil, S. *J. Mater. Chem.* **2012**, *22*, 4450.
(30) Thesen, M. W.; Höfer, B.; Debeaux, M.; Janietz, S.; Wedel, A.; Köhler, A.; Johannes, H. H.; Krueger, H. *J. Polym. Sci., Part A: Polym. Chem.* **2010**, *48*, 3417.
(31) Bagnich, S. A.; Unger, T.; Jaiser, F.; Neher, D.; Thesen, M. W.; Krueger, H. *J. Appl. Phys.* **2011**, *110*, 033724.
(32) Borsenberger, P. M.; Weiss, D. S. *Organic Photoreceptors for Xerography*; Marcel Dekker: New York, 1998.
(33) Borsenberger, P. M.; Gruenbaum, W. T.; Wolf, U.; Bässler, H. *J. Chem. Phys.* **1998**, *234*, 277.
(34) Treacher, K., Stoessel, P., Spreitzer, H., Becker, H., Falcou, A. U.S. Patent Application WO03/048225 A2, 2003.
(35) Ho, P. K. H.; Kim, J. S.; Tessler, N.; Friend, R. H. *J. Chem. Phys.* **2001**, *115*, 2709.
(36) Khan, A. L. T.; Sreearunothai, P.; Herz, L. M.; Banach, M. J.; Köhler, A. *Phys. Rev. B* **2004**, *69*, 085201.
(37) Sakanoue, K.; Motoda, M.; Sugimoto, M.; Sakaki, S. *J. Phys. Chem. A* **1999**, *103*, 5551.

(38) Frisch, M. J. T.; Trucks, G. W.; Schlegel, H. B.; Scuseria, G. E.; Robb, M. A.; Cheeseman, J. R.; Montgomery, J. A., Jr.; Vreven, T.; Kudin, K. N.; Burant, J. C.; Millam, J. M.; Iyengar, S. S.; Tomasi, J.; Barone, V.; Mennucci, B.; Cossi, M.; Scalmani, G.; Rega, N.; Petersson, G. A.; Nakatsuji, H.; Hada, M.; Ehara, M.; Toyota, K.; Fukuda, R.; Hasegawa, J.; Ishida, M.; Nakajima, T.; Honda, Y.; Kitao, O.; Nakai, H.; Klene, M.; Li, X.; Knox, J. E.; Hratchian, H. P.; Cross, J. B.; Bakken, V.; Adamo, C.; Jaramillo, J.; Gomperts, R.; Stratmann, R. E.; Yazyev, O.; Austin, A. J.; Cammi, R.; Pomelli, C.; Ochterski, J. W.; Ayala, P. Y.; Morokuma, K.; Voth, G. A.; Salvador, P.; Dannenberg, J. J.; Zakrzewski, V. G.; Dapprich, S.; Daniels, A. D.; Strain, M. C.; Farkas, O.; Malick, D. K.; Rabuck, A. D.; Raghavachari, K.; Foresman, J. B.; Ortiz, J. V.; Cui, Q.; Baboul, A. G.; Clifford, S.; Cioslowski, J.; Stefanov, B. B.; Liu, G.; Liashenko, A.; Piskorz, P.; Komaromi, I.; Martin, R. L.; Fox, D. J.; Keith, T.; Al-Laham, M. A.; Peng, C. Y.; Nanayakkara, A.; Challacombe, M.; Gill, P. M. W.; Johnson, B.; Chen, W.; Wong, M. W.; Gonzalez, C.; Pople, J. A. *Gaussian03*, revision C. 02.; Gaussian, Inc.: Wallingford, CT, 2004.
(39) Nayyar, I. H.; Batista, E. R.; Tretiak, S.; Saxena, A.; Smith, D. L.; Martin, R. L. *J. Phys. Chem. Lett.* **2011**, *2*, 566.
(40) Mayo, M. L.; Gartstein, Y. N. *J. Chem. Phys.* **2009**, *130*, 134705.
(41) Mayo, M. L.; Gartstein, Y. N. *J. Phys. Chem. A* **2010**, *114*, 6444.
(42) Economou, E. N. *Green's Functions in Quantum Physics*; Springer: New York, 1983.
(43) Blom, P. *Nat. Mater.* **2012**, *11*, 882.
(44) Köhler, A. *Nat. Mater.* **2012**, *11*, 836.
(45) Parris, R. E.; Kenkre, V. M.; Dunlap, D. H. *Phys. Rev. Lett.* **2001**, *87*, 126601.
(46) Novikov, S. V.; Tyutnev, A. P.; Schein, L. B. *Chem. Phys.* **2012**, *403*, 68.
(47) Borsenberger, P. M.; Richert, R.; Bässler, H. *Phys. Rev. B* **1993**, *47*, 4289.
(48) Pope, M.; Swenberg, C. E. *Electronic Processes in Organic Crystals and Polymers*; Oxford University Press: New York, 1999.
(49) Marcus, R. A. *J. Chem. Phys.* **1956**, *24*, 966.
(50) McMahon, D. P.; Troisi, A. *J. Phys. Chem. Lett.* **2010**, *1*, 941.
(51) Norton, J. E.; Bredas, J. L. *J. Am. Chem. Soc.* **2008**, *130*, 12377.
(52) Martinelli, N. G.; Ide, J.; Sanchez-Carrera, R. S.; Coropceanu, V.; Bredas, J. L.; Ducasse, L.; Castet, F.; Cornil, J.; Beljonne, D. *J. Phys. Chem. C* **2010**, *114*, 20678.
(53) Rühle, V.; Lukyanov, A.; May, F.; Schrader, M.; Vehoff, T.; Kirkpatrick, J.; Baumeier, B.; Andrienko, D. *J. Chem. Theory Comput.* **2011**, *7*, 3335.
(54) Fuchs, A.; Steinbrecher, T.; Mommer, M. S.; Nagata, Y.; Elstner, M.; Lennartz, C. *Phys. Chem. Chem. Phys.* **2012**, *14*, 4259.
(55) Borsenberger, P. M.; Bässler, H. *J. Chem. Phys.* **1991**, *95*, 5327.
(56) Bredas, J. L.; Cornil, J.; Heeger, A. J. *Adv. Mater.* **1996**, *8*, 447.
(57) Borsenberger, P. M.; Pautmeier, L. T.; Bässler, H. *Phys. Rev. B* **1992**, *46*, 12145.
(58) Athanasopoulos, S.; Kirkpatrick, J.; Martinez, D.; Frost, J. M.; Foden, C. M.; Walker, A. B.; Nelson, J. *Nano Lett.* **2007**, *7*, 1785.
(59) Sokolov, A. N.; Atahan-Evrenk, S.; Mondal, R.; Akkerman, H. B.; Sanchez-Carrera, R. S.; Granados-Focil, S.; Schrier, J.; Mannsfeld, S. C. B.; Zoombelt, A. P.; Bao, Z. N.; Aspuru-Guzik, A. *Nat. Commun.* **2011**, *2*, 437.
(60) Pai, D. M.; Yanus, J. F.; Stolka, M. *J. Phys. Chem.* **1984**, *88*, 4714.
(61) Fishchuk, I. I.; Kadashchuk, A. K.; Bässler, H.; Weiss, D. S. *Phys. Rev. B* **2002**, *66*, 205208.
(62) Baranovskii, S. D.; Zvyagin, I. P.; Cordes, H.; Yamasaki, S.; Thomas, P. *Phys. Status Solidi B* **2002**, *230*, 281.
(63) Yimer, Y. Y.; Bobbert, P. A.; Coehoorn, R. *J. Phys.: Condens. Matter* **2008**, *20*, 335204.
(64) Ochs, F. W.; Prasad, P. N.; Kopelman, R. *Chem. Phys.* **1974**, *6*, 253.
(65) Laquai, F.; Hertel, D. *Appl. Phys. Lett.* **2007**, *90*, 142109.